Differences in rotational positioning and subsequent distal main branch rewiring of the Tryton stent: An optical coherence tomography and computational study

Differences in rotational positioning and subsequent distal main branch re-wiring of the Tryton stent: an optical coherence tomography and computational study

Maik J. Grundeken[1*], Claudio Chiastra[2*], Wei Wu[2,3], Joanna J. Wykrzykowska[1], Robbert J. De Winter[1], Gabriele Dubini[2], Francesco Migliavacca[2]

1. The Heart Center, Academic Medical Center – University of Amsterdam, Amsterdam, The Netherlands

2. Laboratory of Biological Structure Mechanics, Department of Chemistry, Materials and Chemical Engineering "Giulio Natta", Politecnico di Milano, Milan, Italy

3. Department of Mechanical Engineering, University of Texas at San Antonio, San Antonio, Texas, USA

*The authors contributed equally.

Running title: On the re-wiring of the Tryton stent

Address for correspondence:

Claudio Chiastra, PhD

Laboratory of Biological Structure Mechanics,

Department of Chemistry, Materials and Chemical Engineering "Giulio Natta",

Politecnico di Milano,

Piazza Leonardo da Vinci 32,

20133 Milan, Italy

E-mail: claudio.chiastra@polimi.it

Abstract

Objectives

To evaluate the occurrence of re-wiring through one of the panels of the Tryton stent (instead of the assumed re-wiring in-between the panels) and the influence on stent geometry and mechanics.

Background

Tryton is a side branch stent used in combination with a main branch device. It is placed without the need of rotational orientation. However, it is unknown whether main branch re-wiring accidentally may occur through a panel, instead of in-between the panels.

Methods

We used three-dimensional optical coherence tomography to evaluate the location of distal main branch re-wiring through Tryton. Furthermore, we used computer simulations to evaluate the influence on stent geometry and mechanics.

Results

Re-wiring through a panel (instead of in-between two panels) occurred in 45% of the cases. By using virtual stent deployment, we found minimal differences in ostial side branch stenoses (44.8% in-between the panels and 39.0% through a panel). There were no differences in minimum stent areas of the distal main branch (6.38 mm^2 vs. 6.39 mm^2). In both scenarios, the re-wired Tryton cell was large enough for main branch stenting

(expressed as the diameter of the largest possible circle that fits within the cells): 3.40 mm (in-between the panels) vs. 3.02 mm (through a panel).

Conclusions

In 45% of the Tryton implantations, distal main branch re-wiring (and subsequent main branch stenting) was performed through one Tryton panel, instead of the assumed re-wiring in-between the panels. However, this did not result in unfavorable stent geometries or mechanics, as evaluated with computer simulations.

Keywords

Coronary bifurcation, dedicated stent, intravascular imaging, optical coherence tomography, computer simulation, virtual bench testing

Abbreviations

PCI = percutaneous coronary intervention

3D = three-dimensional

OCT = optical coherence tomography

IFU = instructions for use

POT = proximal optimization technique

FDA = Food and Drug Administration

QCA = quantitative coronary angiography

LAD = left anterior descending coronary artery

D1 = first diagonal branch

RCx = ramus circumflex

RCA = right coronary artery

Introduction

The Tryton Side Branch Stent™ has been developed for a 'simplified culotte' technique with the hope to improve outcomes of percutaneous coronary interventions (PCIs) of bifurcation lesions [1,2]. The Tryton stent shares its proximal part with the main branch stent proximal to the bifurcation. The Tryton stent consists of three zones [1,2]: a proximal main branch zone, the central transition zone, and a distal side branch zone. The proximal main branch zone has two proximal 'wedding bands', from which three undulating fronds connect these wedding bands with three 'panels' of the transition zone. This part of the stent has a minimal amount of metal, resulting in large sized cells, enclosed by the distal margin of the wedding bands, the undulating fronds, and the proximal margins of the panels. The potential benefit of this design is that due to these large sized cells, main branch re-wiring and main branch stent implantation (after Tryton implantation, which is performed first) will become easier and the so called 'napkin ring' effect may be avoided [3,4].

The Tryton stent is placed without (the need of) rotational orientation. However, it is unknown whether main branch re-wiring accidentally may occur through one of the panels, instead of through the large sized cells. Moreover, if this may occur, it is unknown what the impact will be on the mechanical behaviour of the Tryton stent. Therefore, we performed a study using three-dimensional (3D) reconstructions of optical coherence tomography (OCT) pullbacks to evaluate the occurrence *in vivo* of main branch re-wiring through the panels (instead of through the large cells in-between the undulating fronds, distal wedding band and proximal margins of the panels). Furthermore, we performed virtual stent deployment in a bifurcation model to investigate the influence of main branch stent placement through the panels on Tryton stent mechanics.

Methods

Device

The Tryton Side Branch Stent™ is discussed in detail elsewhere [1,2]. Briefly, it is a cobalt-chromium bare metal stent with a strut thickness of 84 μm (0.0033"). It is a slotted-tube, balloon-expandable stent and is 5 or 6 Fr compatible (depending on the size used), delivered using a single rapid exchange system over a conventional 0.014" guidewire. The stent is mounted on a single delivery balloon which is tapered with a larger proximal than distal diameter [1,2].

The Tryton stent consists of three zones. The distal side branch zone has a conventional tubular stent design with out-of-phase zigzag hoops connected with one link per crown. The second zone is the transition zone with three panels that can be independently deformed to adjust to a wide range of bifurcation anatomies. The third zone is the proximal main branch zone which has two 'wedding bands' to mount the proximal part of the stent on the delivery balloon and to 'anchor' the stent in the proximal main branch after implantation. The wedding bands are connected with the panels of the transition zone by three undulating struts. Due to this design there is a minimal amount of metal in the proximal main branch, with a large cell size in-between the most distal wedding band, the undulating struts, and the proximal margin of the panels. This theoretically allows easy delivery of a conventional stent, through the Tryton stent, in the main branch, avoiding problems with deployment of the main branch stent (such as the 'napkin ring' effect).

The stent deployment sequence, as recommended by the manufacturer, is described in the instructions for use (IFU). First, both branches (main and side branch) are wired. Pre-

dilatations of the main branch and/or side branch are performed at the discretion of the operator. Hereafter, the Tryton stent is advanced into the side branch and positioned using the four radio-opaque markers on the stent delivery system [1,2]. The stent is positioned in such a way that the carina lies in-between the two middle markers, without the need for rotational orientation. After stent deployment, it is recommended to perform a proximal optimization technique (POT) by dilatation of the proximal main branch zone to ensure adequate apposition of the wedding bands to the vessel wall. Then, the side branch wire, used for Tryton stent delivery, is retracted and advanced through the Tryton stent into the distal main branch. To avoid re-wiring in-between the Tryton stent cells and the vessel wall, the side branch wire is not further retracted than the proximal main branch zone (proper re-wiring may be further facilitated by leaving the tip of the balloon catheter used for the POT in the proximal main branch; also known as the 'Stella Manoeuvre'). Re-wiring is facilitated by the large sized cells in-between the distal margin of the distal wedding band, the undulating fronds, and the proximal margins of the panels in the transition zone. The 'trapped' main branch wire could then be retracted. Subsequently, a balloon is advanced over the re-wired main branch wire, through the Tryton stent, to pre-dilate the main branch. After dilatation, a conventional tubular stent is advanced, crossing the side branch, and deployed in the main branch. Finally, the side branch is re-wired through the main branch stent and a final kissing balloon dilatation is performed. Ideally, the procedure is finished with a final POT to correct for the oval-shaped stent distortions in the proximal main branch created by overlap of the kissing balloons in the proximal main branch [5].

The stent is commercially available in multiple countries within Europe (CE marked since 2008), Middle East and Africa, and recently the Food and Drug Administration (FDA) granted approval for its use in the United States.

Three-dimensional optical coherence tomography

We used OCT data from two observational studies to evaluate where the Tryton stent was re-wired (through a large sized cell in-between the panels or through a panel). The first study was a follow-up study using quantitative coronary angiography (QCA) and OCT to evaluate the performance of the Tryton stent [6]. All patients provided written informed consent prior to the repeat angiography. In the second study we reported clinical, QCA and OCT data on 10 patients which were treated for bifurcation lesions with the Tryton stent in combination with the Absorb bioresorbable vascular scaffold (BVS) (Abbott Laboratories, Abbott Park, IL, USA) [7]. The necessity to obtain written informed consent was waived by the institutional review committee because the procedures were performed as part of routine clinical care (both devices were CE-marked).

OCT pullbacks were performed with the Ilumien frequency-domain system (St Jude Medical. St Paul, Minnesota, USA). After advancing the OCT imaging catheter over a conventional, 0.014-inch guidewire, pullbacks were performed during continuous X-ray contrast injection of 4 ml/s at a maximum pressure of 300 psi using an injection pump. Images were acquired at 100 frames/s at a pullback speed of 20 mm/s. Calibration was performed based on the reflection of the imaging catheter. From every OCT pullback, each individual strut was detected by hand in each OCT frame. Hereafter, 3D-OCT images were reconstructed offline using the volume rendering software AMIRA (FEI, Hillsboro, OR, USA) [7,8]. For every 3D-OCT

reconstruction, the site of distal main branch fenestration was scored visually by one of the investigators (MJG) as follows:

1. 'in-between two panels', through the large sized cells which are enclosed by the distal wedding band, the undulating fronds and the proximal margin of the panels; and
2. 'through the panel', in which the distal main branch re-wiring was performed through a cell of one of the panels.

Virtual stent deployment

A bifurcation model of the left anterior descending (LAD) coronary artery with its first diagonal (D1) branch was used for the virtual Tryton stent placement. The geometry of the bifurcation model was based on the clinical literature [9]. The lumen diameters of the three branches obeyed Finet's law [10] and were 3.50 mm (proximal main branch), 2.76 mm (distal main branch), and 2.40 mm (side branch), respectively. The distal bifurcation angle was set to 45° while the proximal-to-distal main branch angle was set to 180°. The vessel wall thickness was defined as the 30% of the lumen diameters according to experimental measurements [11]. The vessel wall was divided into three layers, namely intima, media, and adventitia. The material of each layer was modeled using an isotropic hyperelastic constitutive law based on *ex vivo* experimental data on human coronary specimens [11], in accordance with previous studies [12,13].

A validated model of the Tryton stent (length of 19 mm and step delivery system of 2.5 - 3.5 mm) was used. Details of this model are reported elsewhere [14]. Briefly, the cobalt-chromium alloy that characterizes the stent was defined as an elasto-plastic isotropic

material. The polymeric material of the balloon was described by means of an elastic linear isotropic model. Two different elastic moduli were assigned to the proximal and distal parts of the balloon to comply with the manufacturer pressure-diameter relationship. The model of the Tryon stent was validated by comparing an experimental free-expansion with the corresponding computer simulation.

Models of the 3x15 mm Xience V stent (Abbott Laboratories) [13] and NC Sprinter RX non-compliant balloon (Medtronic, Fridley, MN, USA) (sizes 2.5x15 mm, 3x15 mm, and 3.5x9 mm) were also created. All balloon models were calibrated to replicate the manufacturer pressure-diameter curve following the same procedure used for the Tryton step balloon [14].

Two different experiments were performed with virtual stent placements of the Tryton stent in combination with the Xience V stent. The two scenarios were simulated in the bifurcation model using the finite element software ABAQUS/Explicit (Dassault Systèmes Simulia Corp., Providence, RI, USA). Simulation settings were those adopted in previous studies from our group [12,13,15]. In the first virtual stent placement experiment, we assumed an ideal scenario (with re-wiring 'in-between two panels') and the deployment sequence consisted of the following steps, in agreement with the IFU (Figure 1):

1. Insertion of a 19 x 2.5, 3.5 mm Tryton stent in the side branch;
2. Expansion of the Tryton stent at 10 atm;
3. POT by expanding a 3.5x9 mm balloon at 8 atm;
4. Re-wiring from the proximal to distal main branch in-between two panels of the Tryton stent, through one of the large sized cells;

5. Insertion of a 3x15 mm NC Sprinter RX balloon from the proximal to distal main, through the Tryton stent struts;
6. Inflation of this balloon at 8 atm to allow main branch stent delivery;
7. Insertion of a 3x15 mm Xience V in the main branch, through the Tryton stent;
8. Deployment of the Xience V stent (9 atm);
9. Final kissing balloon dilatation by expanding 2.5x15 mm and 3x15 mm NC Sprinter RX balloon balloons at 8 atm in the side branch and main branch, respectively;
10. Finalization of the procedure with a POT by expanding a 3.5x9 mm NC Sprinter RX balloon at 9 atm.

In the second virtual stent placement experiment, we assumed that after Tryton stent placement, one of the panels was located in front of the distal main branch ostium. The deployment sequence and the subsequent steps were identical as described above with the exception that main branch re-wiring (step 4) was performed through one of the panels instead of through the large sized cells in-between two panels (Figure 2).

The two scenarios were compared by quantifying geometrical changes after stenting procedure. The side branch ostial area stenosis (expressed as percentage) was calculated as follows [16]: (total side branch ostium surface area – largest area free from struts) / total side branch ostium surface area * 100. The minimum stent area at the distal main branch ostium was defined as the cross-sectional inner lumen stent area without considering the stent struts [17]. The minimum lumen diameter at the distal main branch ostium was calculated as the cross-sectional minimum diameter from one strut edge to the opposite one [17]. The malapposition area was defined as the percentage of stent area with malapposed stent struts with respect to the total stent area. The geometries of the deployed Tryton

stents were compared by evaluating the cell opening of the large sized cells of the proximal zone and the panels of the transition zone of the device. The diameter of the largest possible circle which fits within the stent cell struts was used as an estimate of the cell opening [17]. In addition to geometrical changes after stenting, the arterial wall stress (expressed as maximum principal stress) and the stress in the stents (expressed as von Mises stress) were calculated as previously reported [18].

Results

Three-dimensional optical coherence tomography

From the 20 patients available, 11 were suitable for the current analysis (Figure 3). In 9 cases it was not possible to assess the location of distal main branch re-wiring. All these cases were from the Tryton OCT follow-up study in which the Tryton stent was used in combination with a metallic stent in the main branch. Therefore, the Tryton stent could not be distinguished from the metallic main branch stent, which prevented 3D-OCT reconstruction of the Tryton stent. One case from this study was suitable for the current analysis since in this case Tryton was used to treat a Medina 0,0,1 lesion without the placement of a main branch stent [19]. Therefore, we were able to 3D reconstruct the Tryton stent during the follow-up OCT, even though it was covered with some neointima. We were able to use all cases (all OCTs were from baseline pullbacks) from the Tryton-Absorb registry, because the metallic Tryton struts could be distinguished from the polymeric Absorb struts.

From these 11 patients, in only 5 (45%) patients main branch re-wiring was performed through the large sized cells, in-between the panels (a case example is shown in Figure 4 and

online video 1). In 5 (45%) other cases, main branch re-wiring was performed through one of the panels (a case example is shown in Figure 5 and online video 2). In the remaining case (9%), main branch re-wiring occurred even further, distal to the panels of the middle zone.

Virtual stent deployment

Figure 6A shows a cross-sectional view of the side branch ostium for the two investigated scenarios. The side branch ostial area stenosis was numerically larger in the case with correct main branch re-wiring (in-between two panels) than in that with main branch re-wiring 'through a panel' (44.8% versus 39.0%, respectively). The minimum stent area at the distal main branch ostium was similar in both scenarios (6.38 mm^2 and 6.39 mm^2 for the cases with correct re-wiring and main branch re-wiring through a panel, respectively) (Figure 6B). Similarly, comparable values of minimum lumen diameter were found at the distal main branch ostium for the two analyzed cases (2.82 mm for both cases).

Malapposed struts are indicated in red in Figure 6C for both scenarios. The malapposition area was numerically smaller in the case with re-wiring in-between two panels (18.7% versus 20.3%, respectively). The percentage of malapposed area at the side branch ostium with respect to the total malapposed area was 19.2% in the case with re-wiring in-between two panels and 14.9% in that with re-wiring through a panel.

In Figure 7 the Tryton stent geometry at the end of the procedure is compared for the two investigated scenarios. The cell opening of the large sized cells of the proximal zone and the panels of the transition zone of the device is reported in Table 1. The assumed main branch re-wiring in-between panels induces a uniform expansion of the stent cells in the proximal and transition zones of the device, with a well-opened large cell in-between the panels

(through which the main branch stent is implanted) with a diameter of the largest possible circle of 3.40 mm (Figure 7, Panel A). Main branch re-wiring through a panel induces a high distortion of one of the panels of the transition zone of the Tryton stent, resulting in a stent cell diameter of 3.02 mm (Figure 7, Panel D), which is approximately three times larger than the other cells of the other panels (Figure 7, Panels E-F). The stent cell diameter of 3.02 mm however is well beyond the 2.76 mm of the distal main branch diameter.

Figure 8A compares the two analyzed cases in terms of stress distribution in the arterial wall at the end of the procedure. In both scenarios, the high stress was confined in the proximal main branch, which was characterized by an overexpansion of the vessel due to kissing balloon inflation. The peak wall stress was localized at the side branch ostium opposite to the carina in both cases and was 0.38 MPa in the case with 'correct' main branch re-wiring and 4.00 MPa in the case with main branch re-wiring 'through a panel'. Figure 8B shows the distribution of stress in the stents, which was similar in both scenarios. The peak stress occurred in the Tryton stent in both scenarios at the crown of the transition zone that is connected with one link to the distal zone and was 629 MPa with 'correct' main branch re-wiring and 619 MPa with re-wiring 'through a panel'.

Discussion

The main findings of the current study are:

1. After Tryton stent implantation, as shown with 3D-OCT, distal main branch re-wiring and subsequently main branch stenting is performed through a Tryton panel (instead of the assumed scenario of re-wiring through the large sized cells in-between the panels) in 45% of the evaluated cases.

2. We evaluated the implications of these two clinical scenarios on mechanical stent behavior using virtual stent deployments and we found differences in stent geometries and mechanical stent behavior between the two different clinical scenarios.
3. The main differences with virtual stent deployment were: a) ostial side branch stenosis of 44.8% ('in-between the panels') versus 39.0% ('through a panel'); b) diameter of the largest possible circle that fit the re-wired stent cells after main branch implantations of 3.40 mm ('in-between the panels') versus 3.02 mm ('through a panel'); and c) peak wall stress which was 0.38 MPa ('in-between the panels') versus 4.00 MPa ('through a panel').

In contrast to other dedicated bifurcation stents, such as the Nile-CroCo or Nile-PAX (Minvasys, Gennevilliers, France) [20], the Tryton stent does not need rotational orientation during implantation. However, when analyzing one of the Tryton stent implantations performed in our catheterization lab (Academic Medical Center, Amsterdam, The Netherlands), using 3D-OCT (the case example of Figure 5, online video 2), we noticed that after Tryton implantation, one of the panels 'blocked' the distal main branch ostium. When carefully analyzing the 3D-OCT reconstruction of the Tryton stent from the main branch pullback after main branch stenting (possible because of the use of Absorb BVS), we noticed that re-wiring and main branch stent placement was performed through one of the panels, instead of the assumed placement through the large cells in-between the panels. Therefore, we have systematically analyzed the occurrence of this phenomenon by evaluating all 3D-OCT reconstructions available from earlier studies. To our surprise, we found an incidence of 45% of 'correct' re-wiring and main branch stent placement (through the large sized cells in-between the panels), and 45% of 'incorrect' placement (through the panels). This posed the question whether this was clinically relevant. However, a clinical

study to investigate this question necessitates the inclusion of hundreds to thousands of patients to have enough power to evaluate clinical outcomes (such as side branch restenosis) and such a study is not feasible.

As an alternative, we used computer simulations to investigate the influence of the 'through a panel' re-wiring on the geometry and mechanical behavior and of the Tryton stent. This methodology, known as 'virtual bench testing', has been widely accepted as a valuable alternative to *in vitro* bench testing [21,22]. The advantages of virtual over traditional bench testing is that it allows the assessment of quantities that are impossible to measure in an experimental bench test environment, such as the stent stress state.

By using virtual bench testing in the current study, we found that the geometrical differences between the two scenarios were only minimal: ostial side branch stenoses were 44.8% (in-between two panels) versus 39.0% (through a panel) and minimum stent areas of the distal main branch ostium were 6.38 mm^2 (in-between two panels) versus 6.39 mm^2 (through a panel). Importantly, in both scenarios there was an adequate cell opening for main branch stenting as the diameters of the largest possible circles that fit the re-wired stent cells after main branch implantations were 3.40 mm (in-between two panels) and 3.02 mm (through a panel), which is sufficient for the 2.76 mm distal main branch diameter. Therefore, it is unlikely that the 'napkin ring' effect will occur in both scenarios [3,4].

Areas of high stent stresses are associated with stent strut fractures [23]. However, the fenestration of the panel in the re-wiring 'through a panel' scenario did not lead to excessive peak stresses of the stent. In both scenarios, the peak stent stresses remained lower than the ultimate tensile strength of the cobalt-chromium alloy (~1 GPa [24]). Thus, the Tryton stent did not break during the implantation steps. Since the panels showed large

deformations in the scenario in which re-wiring was performed through the panel, we would have expected critical stress values in the transition zone. However, peak stress values were comparable in that region in both scenarios. In both scenarios the highest stresses were located at the crown of the transition zone that is connected with one link to the distal zone (in the side branch ostium opposite to the carina) (Figure 8B). It is therefore unlikely that strut fractures will occur more often in the re-wiring 'through panel' scenario after implantation, although formally, this will need a fatigue testing study.

Our paper has several limitations. The clinical OCT data used in this study was obtained in only 11 patients in one center. Our findings may not be generalizable to all procedures performed with the Tryton stent and re-wiring through the panels may occur less frequently. We used an idealized bifurcation model without stenosis. It is conceivable that stenosis and plaque content (lipid-rich plaques versus calcified plaques, for instance) would yield different results. We were not able to investigate the influence of the two scenarios on clinical outcomes directly. For such an analysis, hundreds to thousands of patients are needed. Furthermore, this analysis is complicated by the inability to distinguish the Tryton stent from a metallic main branch stent. We were able to investigate Tryton re-wiring because of the use of BVS as main branch stent. However, with the more recent reports of increased risk of stent thrombosis with BVS [25,26], its use is no longer recommended, which will hamper future *in vivo* studies on Tryton re-wiring.

Conclusions

The Tryton stent is implanted without the need for rotational orientation. However, we found in 11 patients that distal main branch re-wiring and subsequent main branch stent

implantation may occur through one of the Tryton panels, instead of the assumed implantation through the large sized cell of its proximal portion, in-between the panels. This difference in re-wiring resulted in subtle differences in stent geometries and mechanical stent behavior, as evaluated using computational models of stent deployment. Additional studies are needed to investigate whether these differences will influence clinical outcomes on the long-term.

References

1. Grundeken MJ, Stella PR, Wykrzykowska JJ. The Tryton Side Branch Stent™ for the treatment of coronary bifurcation lesions. Expert Rev Med Devices 2013;10:707–16. doi:10.1586/17434440.2013.848165.
2. Grundeken MJ, Généreux P, Wykrzykowska JJ, Leon MB, Serruys PW. The Tryton Side Branch Stent. EuroIntervention 2015;11 Suppl V:V145-6. doi:10.4244/EIJV11SVA33.
3. Hikichi Y, Inoue T, Node K. Benefits and limitations of cypher stent-based bifurcation approaches: in vitro evaluation using micro-focus CT scan. J Interv Cardiol 2009;22:128–34. doi:10.1111/j.1540-8183.2009.00442.x.
4. Murasato Y, Hikichi Y, Horiuchi M. Examination of stent deformation and gap formation after complex stenting of left main coronary artery bifurcations using microfocus computed tomography. J Interv Cardiol 2009;22:135–44. doi:10.1111/j.1540-8183.2009.00436.x.
5. Foin N, Secco GG, Ghilencea L, Krams R, Di Mario C. Final proximal post-dilatation is necessary after kissing balloon in bifurcation stenting. EuroIntervention 2011;7:597–604. doi:10.4244/EIJV7I5A96.
6. Grundeken MJ, Garcia-Garcia HM, Kraak RP, Woudstra P, de Bruin DM, van Leeuwen TG, Koch KT, Tijssen JG, de Winter RJ, Wykrzykowska JJ. Side branch healing patterns of the Tryton dedicated bifurcation stent: a 1-year optical coherence tomography follow-up study. Int J Cardiovasc Imaging 2014;30:1445–56. doi:10.1007/s10554-014-0504-y.
7. Grundeken MJ, Hassell MECJ, Kraak RP, de Bruin DM, Koch KT, Henriques JPS, van Leeuwen TG, Tijssen JGP, Piek JJ, de Winter RJ, Wykrzykowska JJ. Treatment of coronary bifurcation lesions with the Absorb bioresorbable vascular scaffold in combination with the Tryton dedicated coronary bifurcation stent: evaluation using two- and three-dimensional optical coherence tomography. EuroIntervention 2015;11:877–84. doi:10.4244/EIJY14M08_15.
8. Grundeken MJ, Kraak RP, de Bruin DM, Wykrzykowska JJ. Three-dimensional optical

coherence tomography evaluation of a left main bifurcation lesion treated with ABSORB® bioresorbable vascular scaffold including fenestration and dilatation of the side branch. Int J Cardiol 2013;168:e107-8. doi:10.1016/j.ijcard.2013.07.255.

9. Medrano-Gracia P, Ormiston J, Webster M, Beier S, Young A, Ellis C, Wang C, Smedby Ö, Cowan B. A computational atlas of normal coronary artery anatomy. EuroIntervention 2016;12:845–54. doi:10.4244/EIJV12I7A139.

10. Finet G, Gilard M, Perrenot B, Rioufol G, Motreff P, Gavit L, Prost R. Fractal geometry of arterial coronary bifurcations: a quantitative coronary angiography and intravascular ultrasound analysis. EuroIntervention 2007;3:490–8.

11. Holzapfel G, Sommer G, Gasser CT, Regitnig P. Determination of layer-specific mechanical properties of human coronary arteries with nonatherosclerotic intimal thickening and related constitutive modeling. Am J Physiol Heart Circ Physiol 2005;289:H2048–58. doi:10.1152/ajpheart.00934.2004.

12. Morlacchi S, Chiastra C, Gastaldi D, Giancarlo P, Dubini G, Migliavacca F. Sequential structural and fluid Dynamic numerical simulations of a stented bifurcated coronary artery. J Biomech Eng 2011;133:121010. doi:10.1115/1.4005476.

13. Morlacchi S, Chiastra C, Cutrì E, Zunino P, Burzotta F, Formaggia L, Dubini G, Migliavacca F. Stent deformation, physical stress, and drug elution obtained with provisional stenting, conventional culotte and Tryton-based culotte to treat bifurcations: A virtual simulation study. EuroIntervention 2014;9:1441–53. doi:10.4244/EIJV9I12A242.

14. Chiastra C, Grundeken MJ, Wu W, Serruys PW, de Winter RJ, Dubini G, Wykrzykowska JJ, Migliavacca F. First report on free expansion simulations of a dedicated bifurcation stent mounted on a stepped balloon. EuroIntervention 2015;10:e1-3. doi:10.4244/EIJV10I11A226.

15. Iannaccone F, Chiastra C, Karanasos A, Migliavacca F, Gijsen FJH, Segers P, Mortier P, Verhegghe B, Dubini G, De Beule M, Regar E, Wentzel JJ. Impact of plaque type and side

branch geometry on side branch compromise after provisional stent implantation. A simulation study. EuroIntervention 2016. doi:10.4244/EIJ-D-16-00498.

16. Ormiston JA, Webster MWI, Webber B, Stewart JT, Ruygrok PN, Hatrick RI. The "Crush" Technique for Coronary Artery Bifurcation Stenting: Insights From Micro-Computed Tomographic Imaging of Bench Deployments. JACC Cardiovasc Interv 2008;1:351–7. doi:10.1016/j.jcin.2008.06.003.

17. Ng J, Foin N, Ang HY, Fam JM, Sen S, Nijjer S, Petraco R, Di Mario C, Davies J, Wong P. Over-expansion capacity and stent design model: An update with contemporary DES platforms. Int J Cardiol 2016;221:171–9. doi:10.1016/j.ijcard.2016.06.097.

18. Morlacchi S, Colleoni SG, Cárdenes R, Chiastra C, Diez JL, Larrabide I, Migliavacca F. Patient-specific simulations of stenting procedures in coronary bifurcations: two clinical cases. Med Eng Phys 2013;35:1272–81. doi:10.1016/j.medengphy.2013.01.007.

19. Grundeken MJ, Agostoni P, Lesiak M, Koch KT, Voskuil M, de Winter RJ, Wykrzykowska JJ, Stella PR. Placement of Tryton Side Branch Stent only; a new treatment strategy for Medina 0,0,1 coronary bifurcation lesions. Catheter Cardiovasc Interv 2013;82:E395-402. doi:10.1002/ccd.24811.

20. Berland J. The Nile CroCo and Nile PAX stents. EuroIntervention 2015;11 Suppl V:V149-50. doi:10.4244/EIJV11SVA35.

21. Antoniadis AP, Mortier P, Kassab G, Dubini G, Foin N, Murasato Y, Giannopoulos AA, Tu S, Iwasaki K, Hikichi Y, Migliavacca F, Chiastra C, Wentzel JJ, Gijsen F, Reiber JHC, Barlis P, Serruys PW, Bhatt DL, Stankovic G, Edelman ER, Giannoglou GD, Louvard Y, Chatzizisis YS. Biomechanical Modeling to Improve Coronary Artery Bifurcation Stenting: Expert Review Document on Techniques and Clinical Implementation. JACC Cardiovasc Interv 2015;8:1281–96. doi:10.1016/j.jcin.2015.06.015.

22. Migliavacca F, Chiastra C, Chatzizisis YS, Dubini G. Virtual bench testing to study coronary

bifurcation stenting. EuroIntervention 2015;11. doi:10.4244/EIJV11SVA7.

23. Everett KD, Conway C, Desany GJ, Baker BL, Choi G, Taylor CA, Edelman ER. Structural Mechanics Predictions Relating to Clinical Coronary Stent Fracture in a 5 Year Period in FDA MAUDE Database. Ann Biomed Eng 2016;44:391–403. doi:10.1007/s10439-015-1476-3.

24. Poncin P, Millet C, Chevy J, Proft JL. Comparing and optimizing Co-Cr tubing for stent applications. In: Helmus M, Medlin D, editors. Med. Device Mater. II - Proc. Mater. Process. Med. Devices Conf., 2004, p. 279–83. doi:0871708248.

25. Ali ZA, Serruys PW, Kimura T, Gao R, Ellis SG, Kereiakes DJ, Onuma Y, Simonton C, Zhang Z, Stone GW. 2-year outcomes with the Absorb bioresorbable scaffold for treatment of coronary artery disease: a systematic review and meta-analysis of seven randomised trials with an individual patient data substudy. Lancet (London, England) 2017;390:760–72. doi:10.1016/S0140-6736(17)31470-8.

26. Wykrzykowska JJ, Kraak RP, Hofma SH, van der Schaaf RJ, Arkenbout EK, IJsselmuiden AJ, Elias J, van Dongen IM, Tijssen RYG, Koch KT, Baan J, Vis MM, de Winter RJ, Piek JJ, Tijssen JGP, Henriques JPS, AIDA Investigators. Bioresorbable Scaffolds versus Metallic Stents in Routine PCI. N Engl J Med 2017;376:2319–28. doi:10.1056/NEJMoa1614954.

Figures

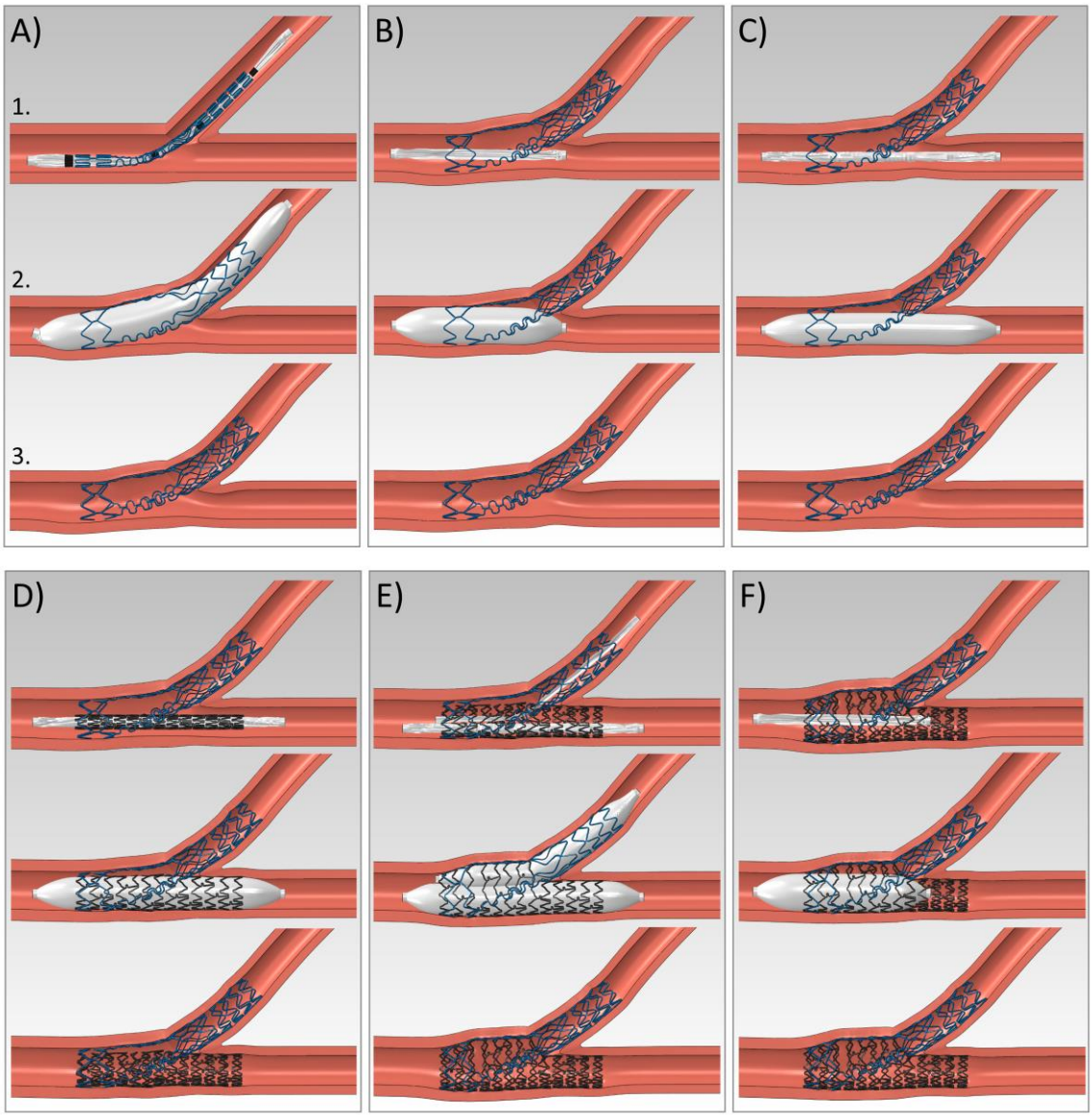

Figure 1. Virtual deployment sequence of the Tryton stent in combination with the Xience V stent in a left anterior descending / first diagonal coronary bifurcation model. **A**: Expansion of the Tryton stent in the side branch. **B**: Proximal optimization technique. **C**: Opening of the main branch access. **D**: Expansion of the Xience V stent in the main branch. **E**: Kissing balloon inflation. **F**: Proximal optimization technique. For each step, (1) insertion, (2) expansion, and (3) recoil of the balloon/stent is shown.

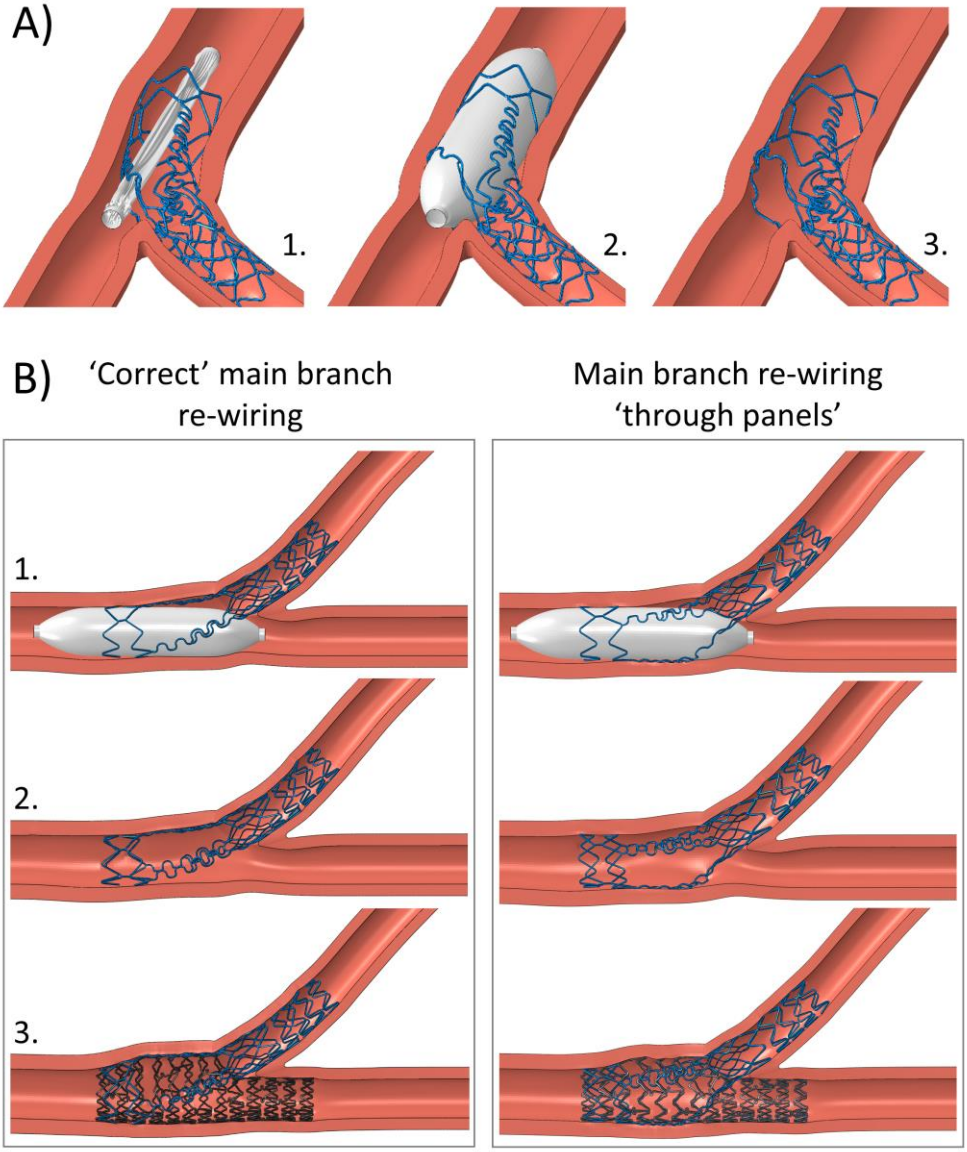

Figure 2. Main branch re-wiring after Tryton stent implantation. **A**: Re-wiring through one of the panels of the stent: (1) insertion of the balloon, (2) expansion, and (3) recoil after balloon deflation. **B**: Comparison between the 'correct' re-wiring and the re-wiring 'through panels': (1) expansion of the balloon, (2) recoil after balloon deflation, and (3) geometrical configuration at the end of the procedure.

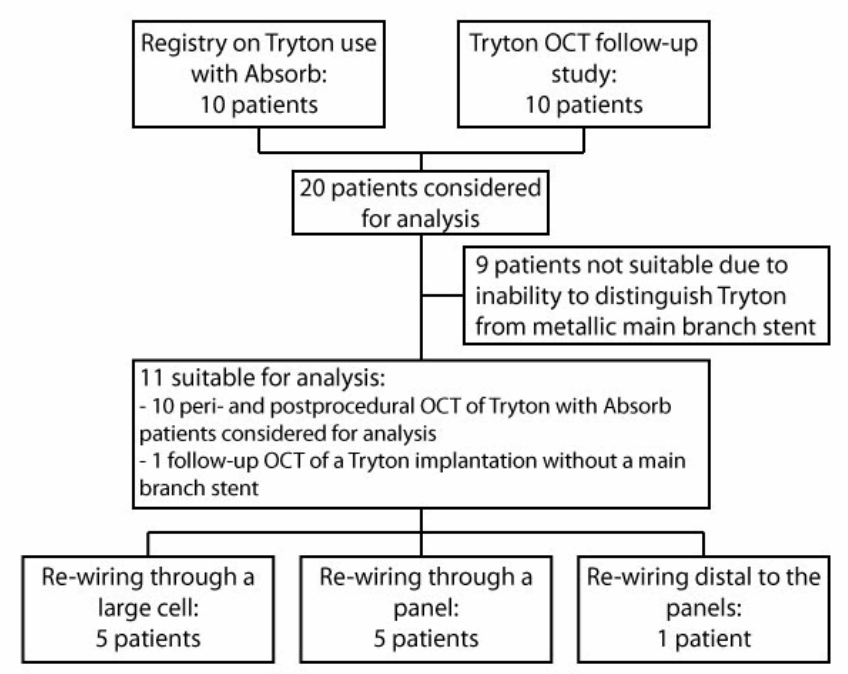

Figure 3. Flowchart reporting the patients included in the analysis.

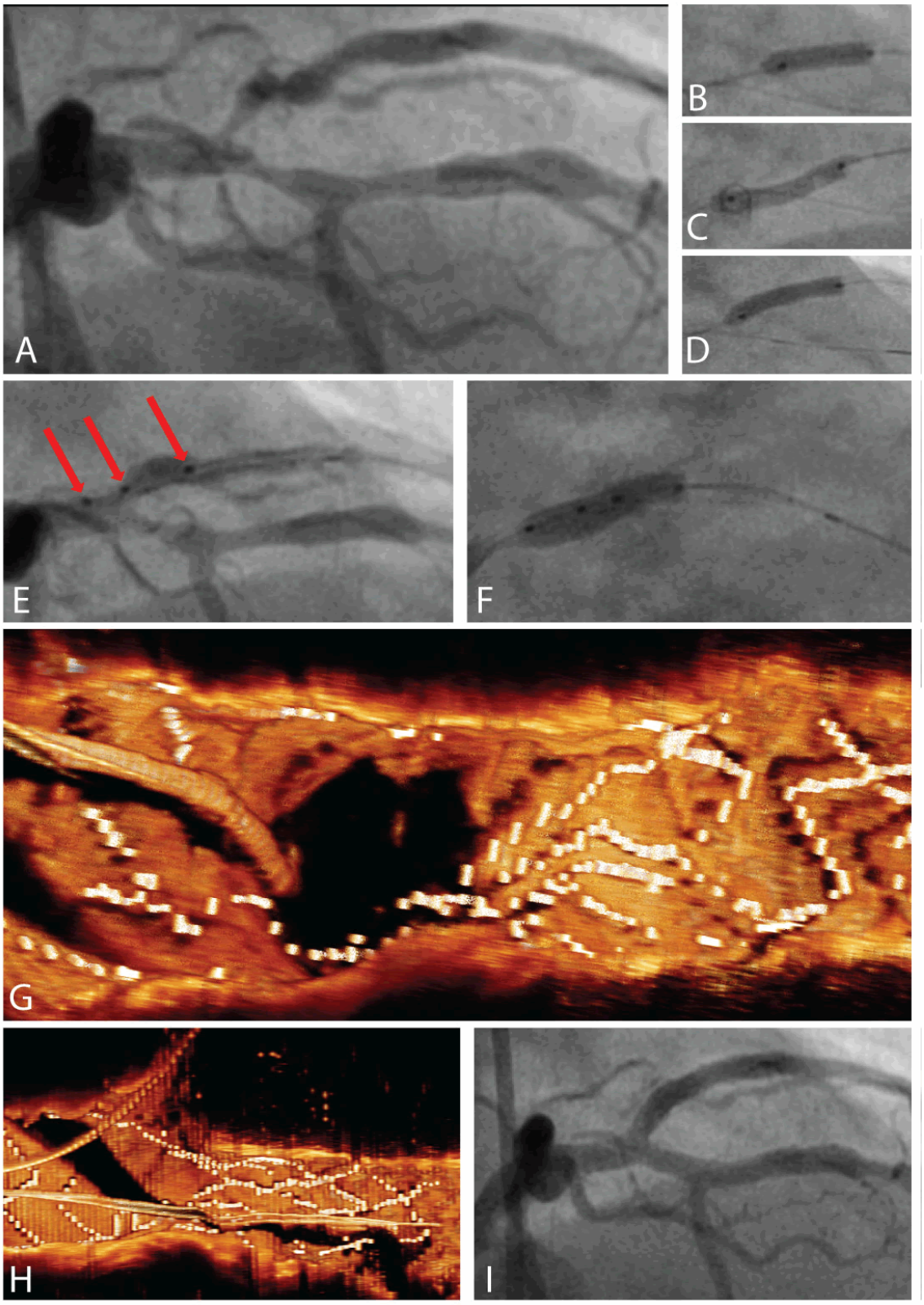

Figure 4. Clinical example of 'correct' main branch re-wiring. This case example was a 53-year-old male with recent STEMI for which he underwent a primary PCI with drug-eluting

stent placement in the ramus circumflex (RCx). **A**: angiography showed a distal LAD lesion and a Medina 1,1,1 lesion of the LAD/D1 bifurcation. The distal LAD was treated with a bioresorbable vascular scaffold (not shown). **B** and **C**: then, the D1 was predilated. **D**: hereafter, an Absorb BVS was implanted in the D1. **E**: a 3.5-3.0×15 mm Tryton was positioned from the proximal LAD into the D1 using the four radiopaque markers on the delivery system (red arrows; most proximal marker not visible). **F**: Tryton was deployed at 10 atm, overlapping with the previously placed BVS. **G**: 3D-OCT reconstruction from a pullback from the side branch to the proximal main branch shows precisely how re-wiring of the guidewire into the distal main branch is in-between the undulating fronds ('correct' re-wiring). **H**: 3D-OCT reconstruction from the same pullback as in 'G', but from a view perpendicular at the distal main branch ostium. **I**: final angiographic result after main branch BVS implantation.

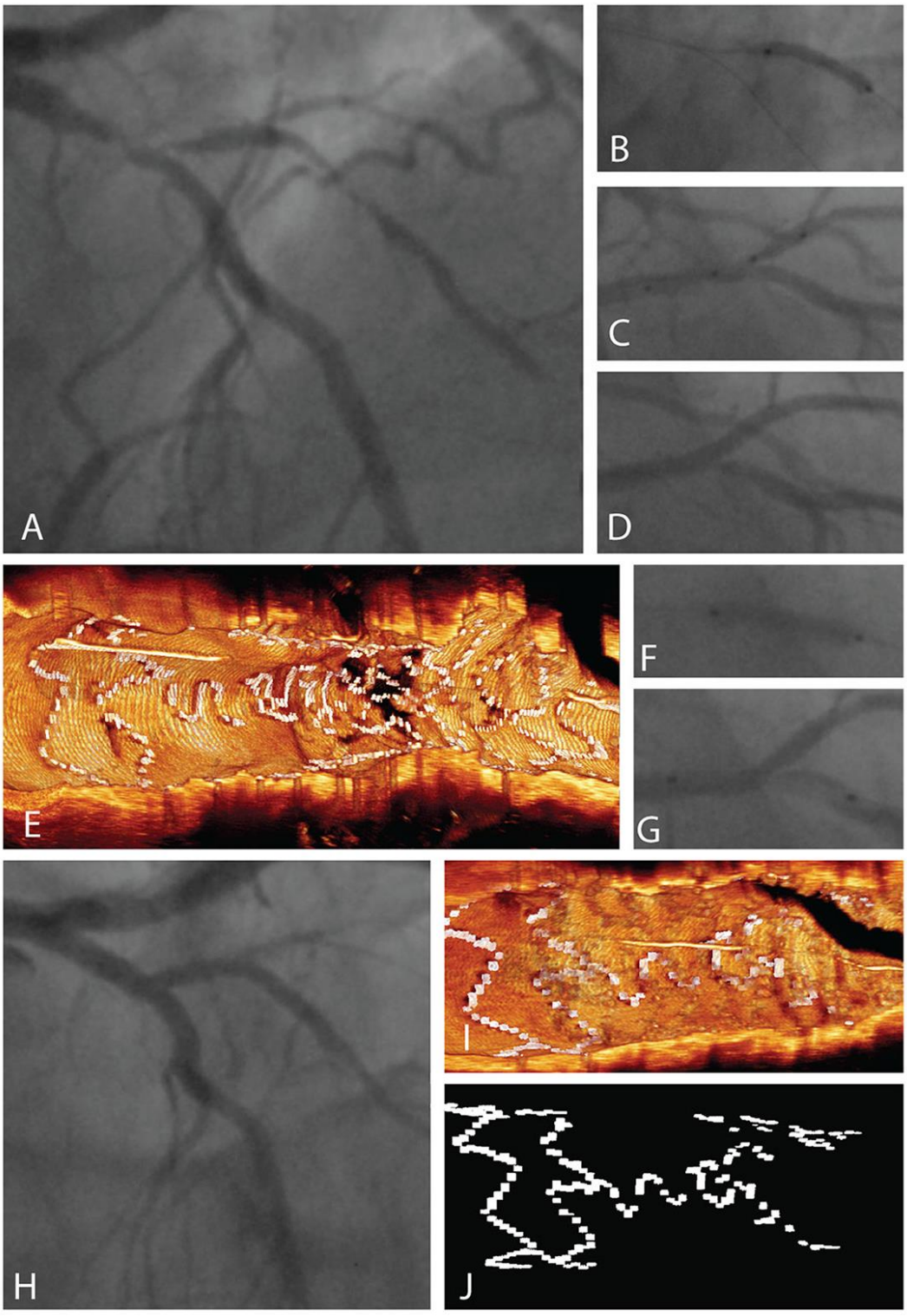

Figure 5. Clinical example of main branch re-wiring 'through a panel'. This case example was a 48-year-old male with a history of PCI of the right coronary artery (RCA) and ramus circumflex (RCx) branch. He presented with progression of his stable angina with an exercise

test suggestive for ischemia in the anterolateral wall. Diagnostic angiography showed a chronic total occlusion of the RCA, patent stents in the RCx (not shown) and, as displayed in panel **A**, a bifurcation lesion of the LAD-D1 branch with a second subtotal stenosis in D1. A PCI was performed. First, both branches were wired. **B**: then, the side branch was treated, after predilatation, with a 2.5×18 mm Absorb BVS. **C**: hereafter, a 3.5-2.5×19 mm Tryton stent was positioned using the four radiopaque markers on the delivery system. Panel **D** show the angiogram after deployment of the Tryton stent. An OCT pullback from the side branch to the proximal main branch was performed. **E**: 3D reconstruction of this pullback shows that one of the three panels of the Tryton stent is located just before the ostium of the distal main branch. **F**: the main branch was re-wired and a main branch balloon dilatation was performed with a 3.0×15 mm NC Trek balloon. **G**: This is followed by implantation of a 3.0×18 mm Absorb BVS (10 atm). Final kissing balloon dilatation was not performed in this case. **H**: the final angiogram shows a good angiographic result. **I**: 3D reconstruction of a final OCT pullback from distal-to-proximal main branch showing how the struts of the panels are widened after main branch dilatation and BVS placement through the panel (BVS struts not colored). **J**: 3D reconstruction of the Tryton stent from the same viewing angle as in panel 'I', now without BVS and without vessel wall behind. Note that the distal side branch part of the Tryton stent could not be visualized in panels 'I' and 'J' because these 3D reconstructions are obtained from a main branch pullback.

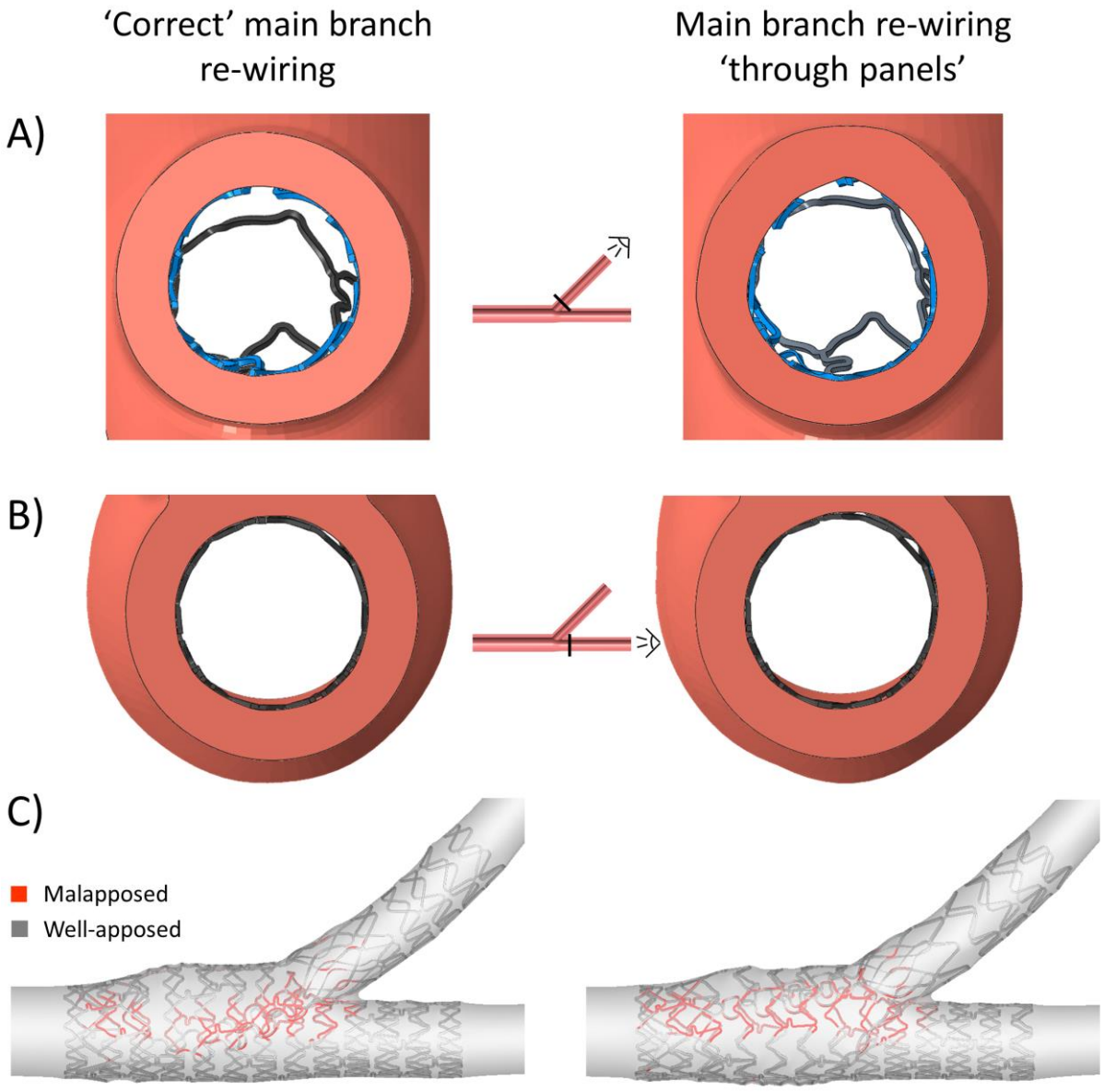

Figure 6. Comparison of the two investigated scenarios in terms of geometrical changes at the end of the stenting procedure. **A**: Cross-sectional view of the side branch ostium from the side branch extremity. **B**: Cross-sectional view of the distal main branch ostium from the distal main branch extremity. **C**: Quantification of stent strut malapposition; malapposed struts are highlighted in red.

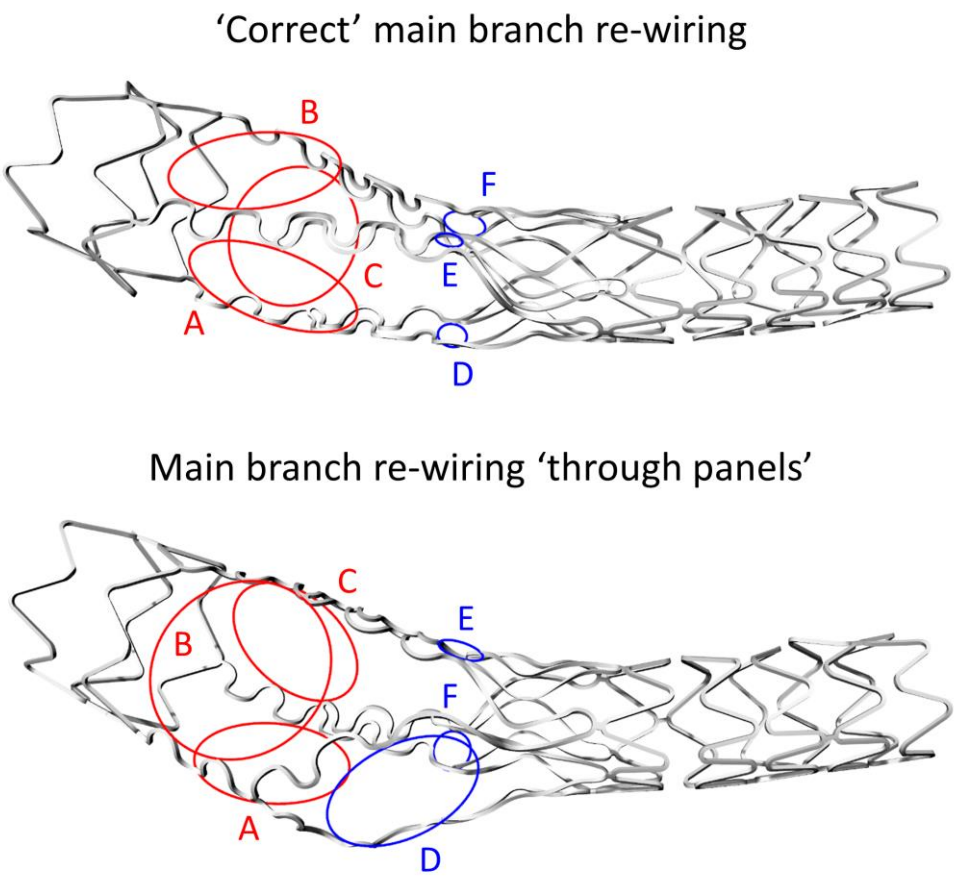

Figure 7. Tryton stent geometry at the end of the procedure for the two investigated scenarios. The circumferences fitted within the large sized cells of the proximal zone (red) and the panels of the transition zone of the stent (blue) were used to estimate the Tryton cells' opening.

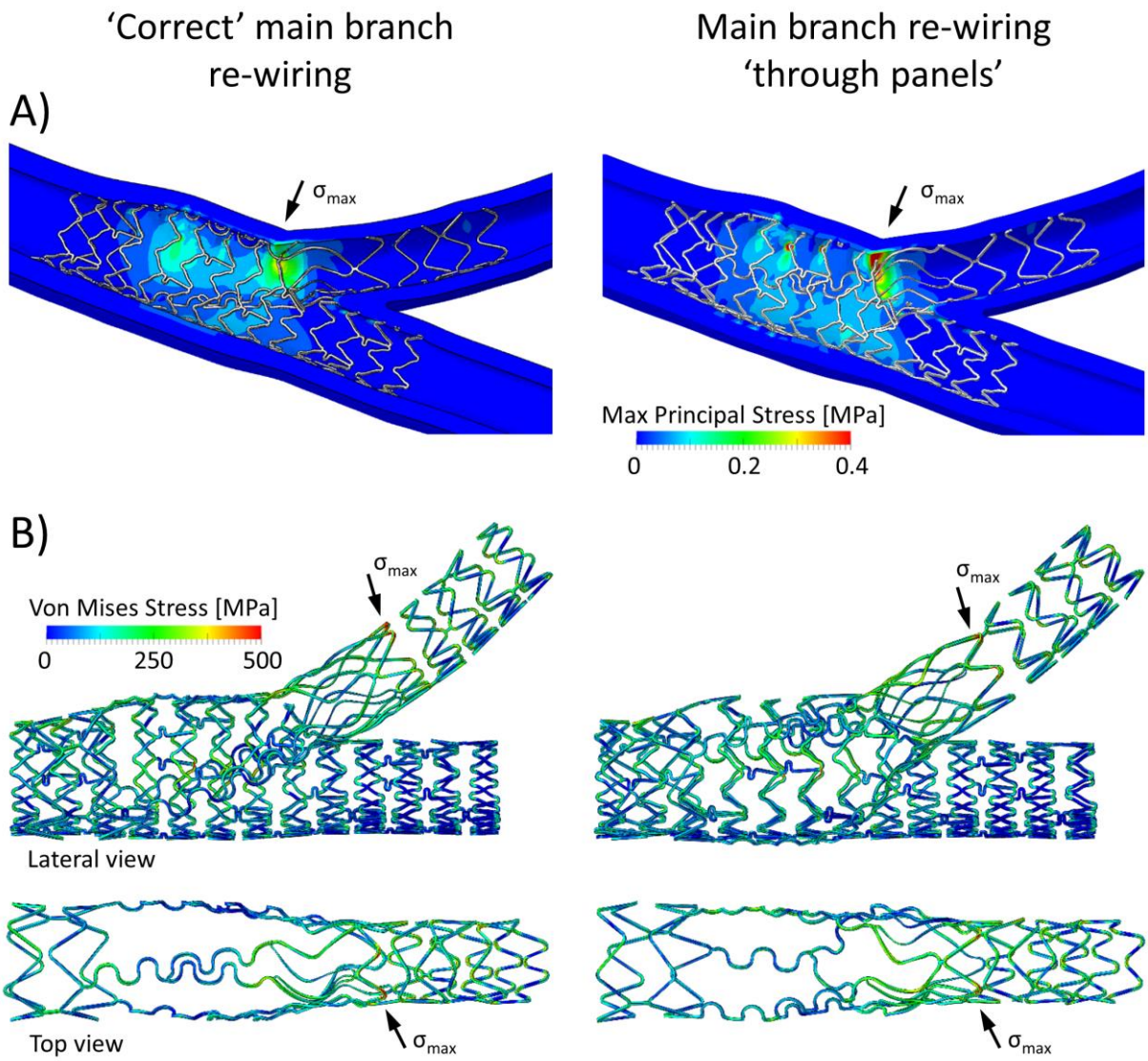

Figure 8. Comparison of the two investigated scenarios in terms of biomechanical outcomes at the end of the stenting procedure. **A**: Contour maps of maximum principal stress in the arterial wall. **B**: Contour maps of von Mises stress in the two deployed stents (top) and in the Tryton stent (bottom). The locations characterized by peak stress are indicated by black arrows.

Supplemental material

Online video 1. Clinical example of 'correct' main branch re-wiring: 3D-OCT reconstruction post stenting procedure.

Online video 2. Clinical example of main branch re-wiring 'through a panel': 3D-OCT reconstruction post stenting procedure.